Proceedings of the Australian Combustion Symposium
November 6-8, 2013, The University of Western Australia

Comparative study of the decomposition of CH_4 in a nonequilibrium plasma and under high temperature pyrolytic conditions

E. M. Kennedy *, S. K. Kundu, V. V. Gaikwad, T. S. Molloy, K. M. King, M. Stockenhuber, J. C. Mackie and B. Z. Dlugogorski
Priority Research Centre for Energy, Faculty of Engineering & Built Environment
The University of Newcastle, Callaghan NSW 2308, Australia

Abstract

In this study, the decomposition of methane in a nonequilibrium plasma, where nitrogen and oxygen were excluded from the feed mixture, was investigated. The major product species formed under conditions where the conversion level of methane was relatively high (up to 50 %) were determined. Hydrogen, acetylene, ethylene, ethane and propane were the primary gaseous species identified, and a liquid fraction was detected, which was characterised by ^{1}H NMR and gel permeation chromatography. The product spectrum formed in the nonequilibrium plasma is compared to the species profile predicted from methane pyrolysis, where the feed composition, residence time and methane conversion levels used in the high temperature pyrolysis simulation matched those in the nonequilibrium plasma experimental reactor.

Keywords: nonequilibrium plasma, methane, pyrolysis.

1. Introduction

Nonequilibrium plasma-assisted combustion is considered to have great potential as a technique to enhance the combustion performance of fuels [1, 2]. One of the main advantages of the plasma is its propensity to generate a high concentration of reactive species, including radicals, ions, and excited species (at low temperatures) which can strongly influence combustion characteristics, especially fuel ignition and lean burn combustion.

From a practical perspective, considerable effort has been afforded to the development of plasma-assisted spark engines, where the plasma leads to faster ignition and flame propagation [3]. Other areas of practical interest include the use of nonequilibrium plasma as a pilot flame in gas turbines [4].

Plasma systems are generally characterised by the extent to which ionic and electronic constituents exist in thermal equilibrium. Systems in thermal equilibrium are typically excited by the continuous application of energy (e.g. stationary arc). Nonequilibrium systems, in contrast, employ methods for restricting the duration of the excitation energy such that thermal effects are temporally skewed or out-of-sync with the excitation. Several practical nonequilibrium excitation methods are described in the literature [5], among those that can be operated at atmospheric pressure include the Pulsed Corona Discharge, Dielectric Barrier Discharge (DBD) and Gliding Arc.

In a DBD system, individual discharge impulses are rapidly self-quenched (i.e. in the order of microsecond duration). The abrupt discontinuity in excitation results in a strongly nonequilibrium plasma. The pulse width is determined by the electrical properties of the dielectric barriers and the magnitude of discharge current rather than by the characteristics of the power supply. As a result, the effective width of individual discharge current impulses depends largely on applied voltage, discharge gap and characteristics of the gas feed. The dielectric barrier reactor is essentially an electrical capacitor in which the dielectric cavity is divided into regions of high and low relative permittivity (i.e. dielectric strength). When a sufficiently high voltage is applied across the dielectric complex the low permittivity region breaks down; the fragmented products from molecules are then available as reactive species [6].

Currently, DBDs have numerous applications, as they integrate the advantages of nonequilibrium plasma properties with the ease of atmospheric pressure operation. Most notably is the use of a DBD reactor commercially to generate ozone, O_3. In addition, DBDs can be operated at reasonably high power levels. DBDs can be constructed in various geometries, depending on the application with planar and cylindrical configurations being the most common.

A study on the decomposition of methane in a nonequilibrium plasma, where oxygen and nitrogen were absent, would assist in revealing the major stable product species. By comparing the plasma experimental results with high temperature methane pyrolysis may disclose the difference and similarities in the key reaction steps involving fuel decomposition which take place in nonequilibrium plasma-assisted combustion of methane.

2. Experimental

2.1 Nonequilibrium plasma

The experimental facility was discussed in detail in our earlier publication [7]. Briefly, a dielectric barrier discharge reactor, constructed out of two

* Corresponding author:
Phone: (+61) 2 9385 4602
Email: s.pasunurthi@unsw.edu.au

concentric dielectric barriers (quartz tubes) was used for this study (Fig. 1). The dielectric tubes have dimensions of 25 mm OD (1.8 mm wall thickness) and 12 mm OD (1.5 mm wall thickness). A helical copper wire (26 mm in length) was used as inner electrode, while a copper shim (20 mm in length), wrapping around the outer tube, was used as the outer electrode. The entire reactor assembly was operated in a dedicated fume cupboard.

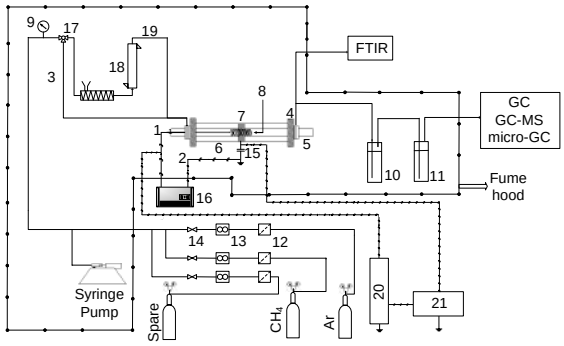

1. High voltage line
2. Ground line
3. Feed gases in
4. Product gases out
5. Inner dielectric
6. Outer dielectric
7. Ground electrode
8. High voltage electrode
9. Pressure gauge
10. NaOH liquid scrubber
11. NaOH solid scrubber
12. Gas filter
13. Mass flow controller
14. Toggle valve
15. Capacitor
16. Reactor power supply
17. 3-way valve
18. Modified solid feeder
19. Feed gases to reactor
20. High voltage probe
21. Oscilloscope

Figure 1: Schematic of DBD reactor assembly and analytical train. Component 18 and syringe pump were not used in the present study. While components 10 and 11 are not important for this study, they help in studying other reactions where acid gases are generated.

The power supply used in the experiments was a voltage resonant topology delivering a sinusoidal AC output voltage of up to 20 kV (rms) at a constant frequency of 21.5 kHz. The voltage figures presented in this article are peak to peak measurements unless otherwise indicated. The power input to the reactor was determined from the enclosed area of voltage-charge Lissajous figure. A sample Lissajous figure is presented in Fig. 2. The calculated input power to the reactor was used to calculate the input energy density (P/F, where P is the average power dissipated by the reactor and F is the total volumetric feed rate). The detail of calculating input energy density can be found elsewhere [8].

A J-type thermocouple was used to measure the temperature of outer electrode (and is considered to be the wall temperature of the outer electrode) in plasma zone where an aliquot of zinc oxide based thermal transfer compound and a mica sheet were used to isolate the thermocouple from the electrical contact while maintaining the thermal contact with the outer electrode.

A GC/MS (Shimadzu QP5000) equipped with AT-Q column was used to identify gas phase products. An online micro-GC (Varian CP-4900), equipped with molesieve 5A and PoraPLOT Q columns, was used to quantify carbon-containing species in both the feed and product flows. A dedicated gas-chromatograph (Shimadzu GC-17A) was used to quantify hydrogen in the product stream.

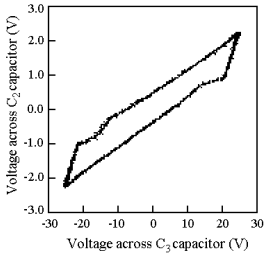

Figure 2: Lissajous figure at 16 kV for a total feed rate of 100 cm^3/min with a CH_4 concentration of 2.5 % (C_3 capacitor sums the reactor displacement charge and C_2 capacitor represents applied voltage of capacitive divider).

The reaction of methane in argon bath gas also results in the production of a liquid hydrocarbon product, and this fraction was analysed by gel permeation chromatograph (GPC) and nuclear magnetic resonance (NMR) spectrometer. In order to produce enough liquid product for analysis by GPC, experiments were conducted over a 4 hour duration. At the end of this period, the high voltage to the DBD was terminated and the reactor was allowed to cool then repeatedly rinsed with tetrahydrofuran (THF) solvent (99.9 %, Merck). The THF/liquid hydrocarbon mixture was then analysed by GPC. For the analysis of the liquid hydrocarbon sample by NMR, a similar experiment was conducted for 4 hours and the reactor tube was rinsed with deuterated chloroform (99.96 atom % D, 0.03% v/v TMS, Aldrich). The deuterated chloroform/liquid hydrocarbon mixture was then analysed by NMR spectrometer.

The GPC employed for this analysis was equipped with a refractive index (RI) detector and three Styragel columns (HR5E, HR3 and HR0.5) operating at 40 °C (manufacturer–Waters, model–GPCV 2000). Polystyrene standards (Polymer Standards Service) with a molecular weight range of 470 to 2300000 g mol^{-1} (M_n) were used for calibration. For NMR experiments, either a Brüker Avance 400 MHz spectrometer or a Brüker Avance 600 MHz spectrometer was used, depending on their availability. For processing of NMR spectra, Brüker Topspin 3.1 software was used.

2.2 Kinetic modelling of CH_4 pyrolysis

The pyrolysis of CH_4 has been widely studied for many years, and detailed kinetic models have been developed in an effort to understand the fundamental reaction chemistry of this process [9]. The auto catalytic nature of the reaction, notably the influence of cyclopentadiene on the reaction rate, has been investigated [10].

In the present investigation, commercial software (Cosilab, version–3.0.3) was used to undertake the kinetic modeling. The GRI-Mech 3.0 [11], which is an optimised mechanism designed to model natural gas combustion, was used for kinetic simulation with all reaction steps involving oxygen or nitrogen removed from the mechanism.

3. Results and Discussion

3.1 Conversion of CH_4 in a nonequilibrium plasma

Figure 3 shows the conversion profile of CH_4 as a function of applied voltage at residence times of 1.48 and 2.95 seconds. As is evident in the figure, the conversion of CH_4 increases with applied voltage. The conversion level of CH_4 reaches 50 % ($\tau = 2.95$ s) and 36 % ($\tau = 1.48$ s) at 16.5 kV. The electrode temperature reaches a maximum temperature 120 °C, which represents the temperature of bulk gas, and highlights how low the gas temperature is in the non equilibrium plasma reactor when compared to the thermal reactor.

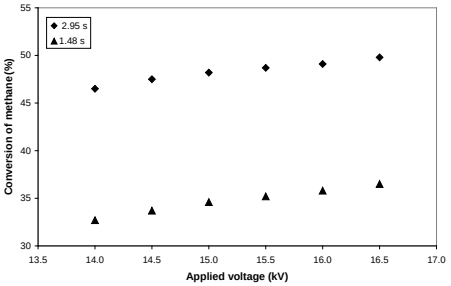

Figure 3: Percentage conversion of CH_4 as a function of applied voltage (feed conditions–2.5 % CH_4 in 100 cm^3/min for $\tau = 2.95$ s and 2.5 % CH_4 in 200 cm^3/min for $\tau =$ □1.48 s).

As the residence time decreases, the conversion of CH_4 drops. This is primarily because the input energy density decreases with a decrease of residence time as can be seen in Fig. 4. Previously, we reported the conversion profile of CH_4 for 9–13 kV [7]. In this article, we report conversion of CH_4 from 14 kV to 16.5 kV.

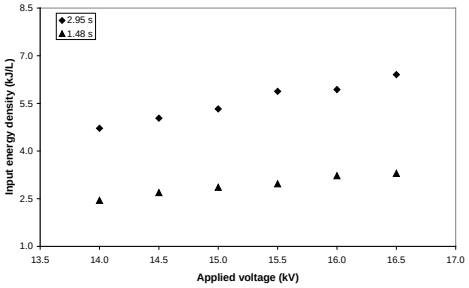

Figure 4: Calculated input energy density as a function of applied voltage.

The conversion of CH_4 in the DBD reactor forms gaseous products including H_2, C_2H_2, C_2H_4, C_2H_6, C_3H_8, *i*-C_4H_{10} and *n*-C_4H_{10}, and liquid and solid hydrocarbon products. Solid hydrocarbons are presumably crosslinked polymeric hydrocarbons. Liquid hydrocarbons are characterised and described in a later section of the paper.

3.2 Kinetic modelling of the conversion of CH_4 at elevated temperatures

The GRI mechanism used in the modeling included 16 species and 40 reactions, and the simulation was undertaken at residence times of 2.95 s and 1.48 s to match the conditions in the DBD experiments. The conversion of CH_4 as predicted from the simulation is presented in Fig. 5. As is evident from the figure, at a temperature of 1050 °C the thermal reactor resulted in a conversion of CH_4 of 25 % at 2.95 s residence time and 19 % at 1.48 s residence time while at 1175 °C the conversion of CH_4 was 70 % at $\tau = 2.95$ s and 59 % at $\tau = 1.48$ s.

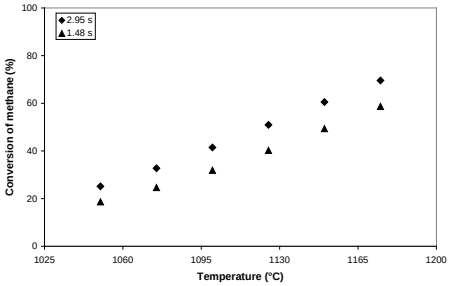

Figure 5: Percentage conversion of CH_4 in thermal reactor as a function of temperature.

3.3 Comparison of gas phase products

The yield of gas phase products has been compared between nonequilibrium plasma and thermal reactor systems and presented in Tables 1 and 2. The conversion value of CH_4 at 16 kV of nonequilibrium plasma has been considered as the reference condition.

Table 1: Comparison of major gaseous products produced in nonequilibrium plasma at 16 kV with their production in thermal reactor at the same level of conversion of CH_4 (49.1 %) at 2.95 s residence time.

	Nonequilibrium plasma experiments	**Thermal pyrolysis model prediction**
H_2 yield	30.8 %	35.4 %
C_2H_2 & C_2H_4 yield	3.94 %	47.7 %
C_2H_6 yield	8.70 %	<1 %
C_3H_8 yield	5.85 %	<1 %
Conditions	Applied voltage: 16 kV, Input energy density: 5.9 kJ/L Reactor temperature: 112 °C	Reactor temperature: 1120 °C

While the yield of H_2 is similar in two systems, the yield level of C_2H_2 and C_2H_4 are significantly higher in thermal reactor. The high yields of C_2H_2 and C_2H_4 in the thermal system and the auto-catalytic nature of the reaction, leads to the formation aromatic products, as reported by Dean [10]. In nonequilibrium plasma system, little or no aromatic species have been observed either in the gas phase product profile or in liquid products. In addition, the yields of C_2H_6 and C_3H_8 are higher in nonequilibrium plasma.

Table 2: Comparison of major gaseous products produced in nonequilibrium plasma at 16 kV with their production in thermal reactor at the same level of conversion of CH_4 (35.8 %) at 1.48 s residence time.

	Nonequilibrium plasma experiments	**Thermal pyrolysis model prediction**
H_2 yield	18.2 %	25.6 %
C_2H_2 & C_2H_4 yield	4.27 %	34.7 %
C_2H_6 yield	8.01 %	<1 %
C_3H_8 yield	4.96 %	<1 %
Conditions	Applied voltage: 16 kV, Input energy density: 3.2 kJ/L Reactor temperature: 112 °C	Reactor temperature: 1112 °C

3.4 Formation of liquid hydrocarbons from nonequilibrium plasma

The thermal reactor produces black carbon particulate product as reported by Wullenkord et al. [12], and the nonequilibrium plasma produces solid and liquid hydrocarbons in addition to gaseous products. In this article, we have characterised the liquid hydrocarbon products by GPC and NMR. Solid hydrocarbon product characterisation is part of our ongoing research.

A typical GPC trace of the liquid product produced in the nonequilibrium plasma is presented in Fig. 6. The sample of liquid hydrocarbons can be split into two groups in GPC analysis. The number average molecular weights (M_n) of them are 480 and 290 g mol^{-1} (polydispersity index of both fractions are nearly 1.1).

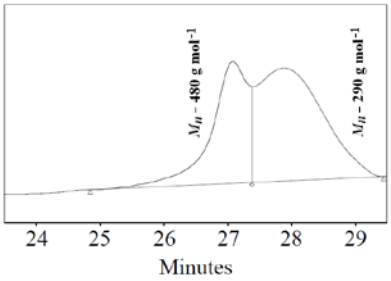

Figure 6: GPC trace of liquid hydrocarbons produced from the reaction of CH_4 in an argon bath gas applying nonequilibrium plasma (applied voltage – 16 kV, feed conditions–2.5 % CH_4 in 100 cm^3/min).

The ^1H NMR spectrum (Fig. 7) highlights the presence of a number of functional groups in the liquid. The peak at approximately 0.86 ppm indicates the presence of a CH_3 group in the liquid [13]. Signals most likely to be the result of protons belonging to CH_2 group can be identified from the peak at 1.25 ppm [13]. The peak at about 1.55 ppm can be attributed to the presence of a CH group in the hydrocarbon liquid [13]. Since the liquid is a mixture of a number of hydrocarbon species, the possibility of overlapping peaks in the ^1H NMR cannot be ruled out. The NMR spectrum also depicts a possibility of unsaturation to be present in the liquid. The peaks around the region of 2 ppm and 5 ppm are suggestive of the presence of unsaturation in the liquid product phase [13].

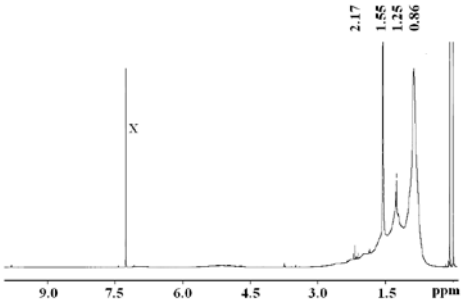

Figure 7: ^1H NMR spectrum for the liquid hydrocarbon mixture (applied voltage–16 kV, feed conditions–2.5 % CH_4 in 100 cm^3/min). The peak marked X at 7.3 ppm is due to the solvent.

Researchers have made several attempts to convert methane to higher hydrocarbons employing various techniques [13-16]. Irrespective of whether an oxidative or a non-oxidative atmosphere is employed for this conversion, the spectrum of products obtained in the liquid fraction is large and complex, making it very difficult to analyse [13-16].

4. Conclusion

The decomposition of methane has been conducted in a nonequilibrium plasma and compared with high temperature methane pyrolysis via simulation. The reaction of methane in nonequilibrium plasma produces liquid hydrocarbons while this product is absent in conventional thermal reactor. The lack of unsaturated products in the nonequilibrium plasma, even under conditions where the conversion levels of CH_4 are high, is a notable difference with the product profile obtained under pyrolytic conditions.

5. Acknowledgements

The authors gratefully acknowledge funding from the Australian Research Council, with additional assistance from the University of Newcastle for Postgraduate Research Scholarships of S. K. Kundu and V. V. Gaikwad.

6. References

[1] A. Starikovskiy and N. Aleksandrov, Prog. Energy Combust. Sci. 39 (1) (2013), pp. 61–110.

[2] S. Wenting and J. Yiguang, J Plasma Fusion Res 89 (4) (2013), pp. 208-219.

[3] S. Stepanyan, É. Polytechnique and G. Vanhove, 51st AIAA Aerospace Science Meeting, AIAA-2013-1053, Grapevine, Texas, 2013.

[4] S. Serbin, 49th AIAA Aerospace Science Meeting, AIAA-2011-61, Orlando, Florida, 2011.

[5] A. A. Fridman, Plasma Chemistry, Cambridge University Press, New York, 2008.

[6] U. Kogelschatz, Plasma chemistry and plasma processing 23 (1) (2003), pp. 1-46.

[7] S. K. Kundu, E. M. Kennedy, V. V. Gaikwad, T. S. Molloy and B. Z. Dlugogorski, Chemical Engineering Journal 180 (15) (2012), pp. 178-189.

[8] S. K. Kundu, E. M. Kennedy, J. C. Mackie, C. I. Holdsworth, T. S. Molloy, V. V. Gaikwad and B. Z. Dlugogorski, Plasma Process. Polym. (2013), DOI: 10.1002/ppap.201300053.

[9] M. S. Khan and B. L. Crynes, Ind. Eng. Chem. 62 (10) (1970), pp. 54-59.

[10] A. M. Dean, J. Phy. Chem. 94 (4) (1990), pp. 1432-1439.

[11] GRI-Mech 3.0, website, http://www.me.berkeley.edu/gri_mech/version30/text30.html [Accessed: 18 Aug 2013].

[12] M. Wullenkord, K.-H. Funken, C. Sattler, R. Pitz-Paal, D. Stolten and T. Grube, 18th World Hydrogen Energy Conference, Essen, Germany, 2010.

[13] G. Scarduelli, G. Guella, I. Mancini, G. Dilecce, S. De Benedictis and P. Tosi, Plasma Processes and Polymers 6 (1) (2009), pp. 27-33.

[14] L. Y. Chen, L. W. Lin, Z. S. Xu, X. S. Li and T. Zhang, Journal of Catalysis 157 (1) (1995), pp. 190-200.

[15] L. D. Conde, C. Marún, S. L. Suib and Z. Fathi, Journal of Catalysis 204 (2) (2001), pp. 324-332.

[16] N. A. S. Amin and D. D. Anggoro, Fuel 83 (4) (2004), pp. 487-494.